coatings

MDPI

Review

Ni-P Coatings as Hydrogen Permeation Barriers—A Review

Deborah Biggio, Bernhard Elsener and Antonella Rossi *

Dipartimento di Scienze Chimiche e Geologiche, Università di Cagliari, Cittadella Universitaria di Monserrato, 09042 Cagliari, Italy; deborah.biggio@unica.it (D.B.); bernhard.elsener@unica.it (B.E.)
* Correspondence: rossi@unica.it

Abstract: Hydrogen became one of the most studied energy carriers after the global energy crisis and can replace gas and oil as clean fuels. The main challenge is its safe storage and long-distance transportation: steel is among the materials most used for hydrogen storage and transportation. However, steel is susceptible to hydrogen embrittlement (HE). HE can be prevented by depositing hydrogen barrier coatings on the steel surface. This review provides an overview of the hydrogen permeation mechanism and the analytical methods employed to evaluate the performance of the hydrogen permeation barriers. The focus is on Ni and electroless Ni-P coatings deposited on steel as hydrogen barriers. These coatings have been used so far for their anti-corrosion and wear properties; they are currently of interest due to their low hydrogen permeability. The simplicity of production and the possibility of achieving a homogeneous coating, regardless of the geometry of the substrate, make the electroless deposition process of the Ni-P alloy a candidate for 'in situ' applications in existing pipelines. This process can be implemented by using and adapting the established pig batch technology.

Keywords: electrochemical permeation test; hydrogen permeability; hydrogen permeation barriers; nickel; Ni-P coating; analytical techniques

Academic Editor: Raul Arrabal

Received: 28 February 2025
Revised: 14 March 2025
Accepted: 18 March 2025
Published: 21 March 2025

Citation: Biggio, D.; Elsener, B.; Rossi, A. Ni-P Coatings as Hydrogen Permeation Barriers—A Review. *Coatings* **2025**, *15*, 365. https://doi.org/10.3390/coatings15040365

1. Introduction

The reliability of energy storage technology is currently of utmost importance for the global energy transition and for stabilizing the supply from renewable energy sources [1]. Hydrogen became one of the most investigated energy carriers after the global energy crisis of 1974: "green hydrogen" can be easily generated by electrolysis from renewable sources, and it can replace gas and oil as a clean fuel, becoming the primary energy carrier in the future [2–5]. The main problem to be solved is the safe storage and long-distance transportation of hydrogen due to hydrogen embrittlement of high-strength steel [6,7]. This problem has become the driving force behind research into new materials for use as hydrogen permeation barriers [8,9]. Steel alloys, as structural materials, are characterized by high strength and durability, good performance, and reasonable cost, and for these reasons, they are widely used in different industrial applications [10–12]. In the gas pipeline and hydrogen technology field, for example, the predominant choice of materials involves using low alloy steel with different carbon contents and heat treatments [13]. However, it is well-known that hydrogen in steel reduces the ductility and formability of the steel [14–18]. Hydrogen in steel can originate from the manufacturing process, corrosion, or its interaction with the surrounding medium. The very small hydrogen atoms can easily be absorbed and pass through the crystal microstructure of the steel by diffusion, causing hydrogen embrittlement (HE) [14,19–25]. The diffusion mechanism of hydrogen entry into the material (e.g., steel) depends on several factors, such as temperature, pressure,

the electrochemical potential at the electrolyte–metal interface, the pH, the composition of the electrolyte, composition of the material, the presence of promoters and inhibitors, and the current density of hydrogen evolution [26]. Diffusion constitutes a phase of a complex process called hydrogen permeation (see the following paragraph) [9].

Electroless Ni-P coatings are commonly used due to their anti-corrosion and anti-wear properties [27–33] and they are currently of interest as hydrogen permeation barriers (HPBs) [34,35]. This review aims to provide an overview of the mechanism of hydrogen permeation and of the analytical methods that can be applied to evaluate the performance of HPBs. It also describes the production and properties of electroless Ni-P coatings with a focus on their application as hydrogen permeation barriers.

2. Hydrogen Permeation Mechanism

Although the mechanism of hydrogen embrittlement is not completely clear, it certainly involves the diffusion of hydrogen atoms [9,36–38]. The hydrogen permeation mechanism can be depicted as a multistep process [39–41]: adsorption, dissociation, dissolution, diffusion, recombination, and desorption. First, the hydrogen molecule is adsorbed onto the surface and dissociated into hydrogen atoms. Second, hydrogen diffuses through the coating (hydrogen permeation barrier) and the substrate. Third, hydrogen atoms desorb after crossing the bi-layer and recombine to form hydrogen molecules (Figure 1a) or are oxidized to a proton (Figure 1b). Various factors influence hydrogen permeation, including vacancies, dislocations, and grain boundaries. These lattice defects can potentially serve as hydrogen traps. Hydrogen trapping occurs when negative trapping energies are measured. This indicates that the hydrogen atom in the potential well of the trap is more stable, resulting in a decrease in H-diffusivity [39–42].

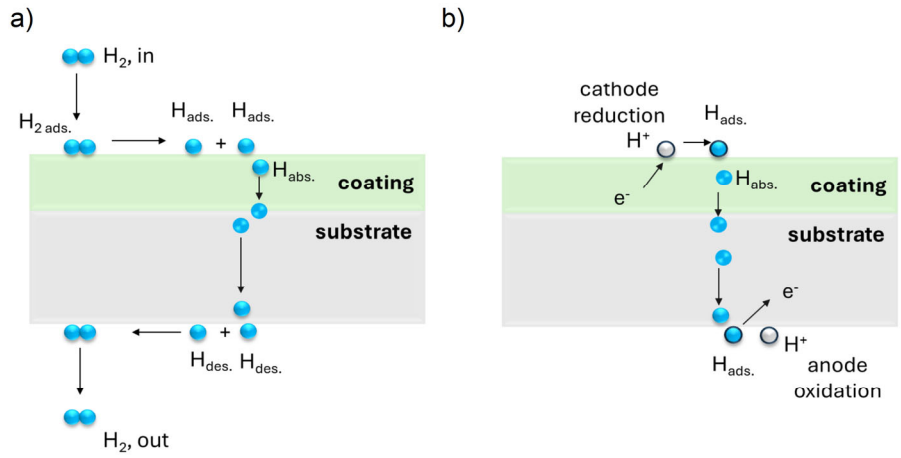

Figure 1. The permeation procedure of hydrogen in a bi-layer system coating/substrate: (**a**) HP mechanisms in gas tests, adapted from [41]; (**b**) HP mechanisms in electrochemical tests.

2.1. Hydrogen Permeability

Hydrogen permeability (P_m), expressed as [mol H_2/(m s Pa0.5)], is the product of effective diffusion (D_{eff}) and solubility (S) [40]. It is calculated from the diffusion constant (D_0), the solubility constant (S_0), the activation energy diffusion (E_D), and the standard enthalpy of dissolution (ΔH_S) for hydrogen as well as the gas constant (R) and temperature (T) [8,43]:

$$P_m = D_{eff} \cdot S = D_0 S_0 e^{-\left(\frac{\Delta H_S + E_D}{RT}\right)} \quad (1)$$

Thus, hydrogen permeability is governed by hydrogen diffusion and the thermodynamic equilibrium and is independent of the surface condition. However, experimental

data on hydrogen permeability reported in the literature indicate that it is strongly influenced by various properties of the surface sample [44]. Equation (1) considers the hydrogen diffusion and its dissolution into the lattice but neglects the trapping effects and the influence of the defects within the material [44].

Hydrogen diffusion flux (J) (mol m^{-2} s^{-1}) for an ideal homogenous single crystal, without any lattice defects, may be derived from Fick's first (Equation (2)) and second (Equation (3)) laws [8,26,45]:

$$J = -D_{eff} \cdot \frac{\delta C}{\delta x} \quad (2)$$

$$\frac{\partial C}{dt} = {D_{eff}}^2 \cdot \frac{\delta^2 C}{\delta x^2} \quad (3)$$

where D_{eff} is the effective diffusion constant, C the concentration of diffusible hydrogen and x the distance vertical to the surface; thus, dc/dx is the gradient of the hydrogen concentration in the permeation direction in the metal membrane [14], and t is the time.

The situation for a bi-layer coating/substrate has been solved by Song [46]. Equations (2) and (3) can be written for both layers, substituting D_{eff} with D_1 and D_2, respectively. As the flux through both layers must be the same, at the boundary between the two layers holds Equation (4), and the relation between the effective diffusion coefficient of the bi-layer D_{eff} and D_1 and D_2 is calculated [46].

$$D_1 \cdot \frac{\delta C_1}{\delta x} = D_2 \cdot \frac{\delta C_2}{\delta x} \quad (4)$$

2.2. Electrochemical Method for Evaluating the HP: Devanathan–Stachurski's Cell

Several methods are reported in the literature, such as the gaseous hydrogen permeation method [47,48]; the dynamic method, which involves applying a quadrupole mass spectrometer (QMS) [49]; the static method, which involves recording the pressure rise in an accumulation volume by an inert pressure gauge [44] and can be used for evaluating hydrogen permeability (HP); and the electrochemical method. The electrochemical method provides information not only concerning diffusion constants, but also on the density of trap sites and their associated energies [8,50]. An instrument for measuring hydrogen permeability is called Devanathan–Stachurski's (D-S) cell [50,51] (Figure 2). It is a dual electrochemical cell configuration, with reference electrodes (RE) (e.g., Ag/AgCl), counter electrodes (CE) (platinum grid) and a thin metal sample between the two cells that acts as the working electrode (WE). Each electrochemical cell is connected to a potentiostat. This set up accurately determines the hydrogen permeation rate [50,51].

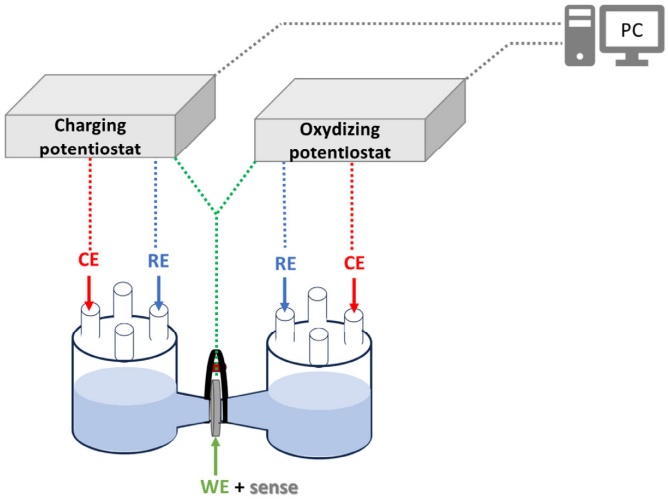

Figure 2. Scheme of Devanathan–Stachurski's cell.

In the cathode cell, H_2 is produced: for this reason, this cell is also known as a production cell. The atomic hydrogen passes through the tested sample (WE), and the hydrogen permeation current is recorded in the anode cell (detection cell), obtaining the hydrogen permeation curve (Figure 3).

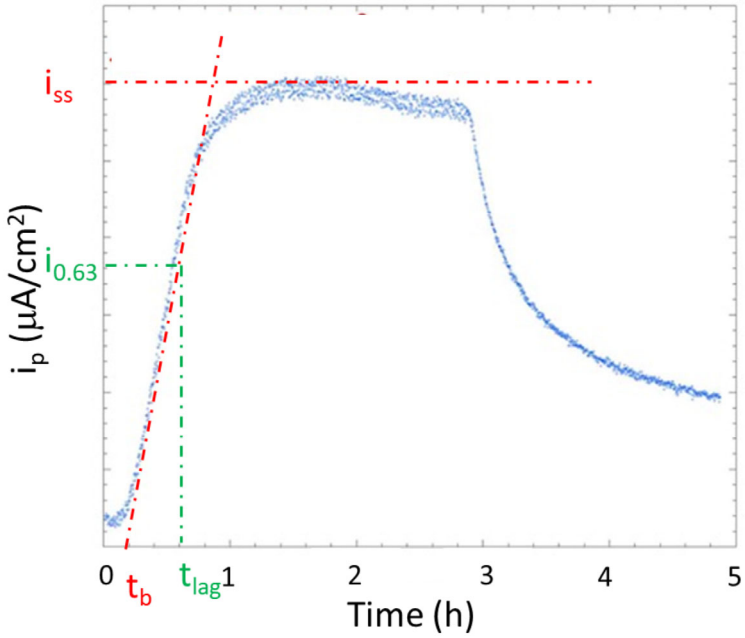

Figure 3. Example of a hydrogen permeation curve (blue line) obtained using ARMCO iron. Red line: determination of the steady-state current (i_{ss}) and breakthrough time t_b. Green line: determination of the permeation current reaches 0.63 times the steady-state ($i_{0.63}$) current and the retardation time t_{lag}.

The configuration of the cell and the standard procedure are reported in the ASTM 148-97(2018) [52] and in the ISO 17081:2014 [53]. The optimal geometric model and boundary conditions for accurately measuring the diffusion coefficient of hydrogen in metals are as follows:

- A membrane with a fixed thickness, x = L, is being considered where the in-plane dimensions y and z are significantly larger than L;
- The concentration of hydrogen atoms at the production side of a membrane remains constant over time, and the concentration is zero on the detection side, i.e., $C = C_0$ at x = 0 and C = 0 at x = L for any value of the time t.

The hydrogen flow at the detection side can be derived as a function of the time as outlined in references [26,54,55] and a mathematical model for the anodic flux in a D-S cell over time is developed. From the hydrogen permeation curve (Figure 3), the effective hydrogen diffusion coefficient can be calculated for a single material or a bi-layer by the following equations [50,51]:

$$D_{eff} = L^2/15.3\ t_b \quad (5)$$

$$D_{eff} = L^2/6\ t_{lag} \quad (6)$$

where D_{eff} is the effective hydrogen diffusion coefficient in m^2/s; L is the thickness of the sample in meters; t_b is the breakthrough time (corresponding to the intersection of the tangent line at the inflection point and the horizontal axis in the curve) in seconds; and t_{lag} is the retardation time: i.e., the time when the permeation current reaches 0.63 times the steady-state current value in seconds (Figure 3). To estimate the diffusion coefficient of the coating, Equation (9) in Section 3.5 has to be considered.

Moreover, it is possible to determine the subsurface concentration of hydrogen C_0 (in ppm) by using the following relationship [56,57]:

$$C_0 = \frac{i_{ss} L}{F D_{eff}} \frac{M_H}{\rho_{Fe}} 10^6 \quad (7)$$

where,

i_{ss}: is the steady state permeation current density (A/m^2),
L: is the thickness of the sample (m),
D_{eff}: is the effective diffusion coefficient (m^2/s),
F: is the Faraday constant (96,485 C/mol),
M_H: is the molar mass of hydrogen (1 g/mol),
ρ_{Fe}: is the iron density (7.87×10^6 g/m^3).

3. Hydrogen Permeation Barriers

3.1. General

Typically, hydrogen storage tanks or pipelines are made of steel that can suffer hydrogen embrittlement (HE). HE can be prevented by depositing a hydrogen barrier coating (HPB) on the steel substrate [9,38]. An efficient hydrogen permeation barrier should prevent or reduce the hydrogen adsorption and should have no structural defects, such as pinholes, pores or cracks. While D_{eff} and C_0 describe the hydrogen diffusion process, the HPB efficiency can be assessed by the permeation reduction factor (PRF) [44]. The PRF is the steady-state ratio of the permeation rate through the uncoated substrate $j_{uncoated}$ divided by the permeation rate through the coated substrate j_{coated} (Equation (8)):

$$PRF = \frac{j_{uncoated}}{j_{coated}} \quad (8)$$

In the case of a multilayer system with both substrate and coating, the PRF value can be used to estimate the coating permeability P_{coat} according to Equation (9), taking into account the thickness and the permeability of the substrate, L_{steel} and P_{steel}, respectively, and the thickness of the coating, L_{coat} [58]. The permeability of the substrate is estimated from separate experiments as $P_{steel} = D_{steel} \times C_{0\,steel}$ (Equations (6) and (7)).The higher the value of PRF, the better the HPB [44,58].

$$PRF \cong \frac{L_{coat} P_{steel}}{L_{steel} P_{coat}} \quad (9)$$

Different coatings have been tested as hydrogen barriers [58]. Ceramic coatings are widely studied as HPBs due to their high-temperature suitability and corrosion resistance properties, which are important in the hydrogen environment [44,58–61]. The PRF value might vary from 236 for a Cr_2N coating to 4600 in the case of ZrN (Figure 4) [44,59,60,62,63]. Although the PRF value is an indicator of the coating's efficiency and of the application potential of the barrier, it is not a sufficient value as it does not consider other aspects such as the adherence to and the suitability of the coating for the substrate [58].

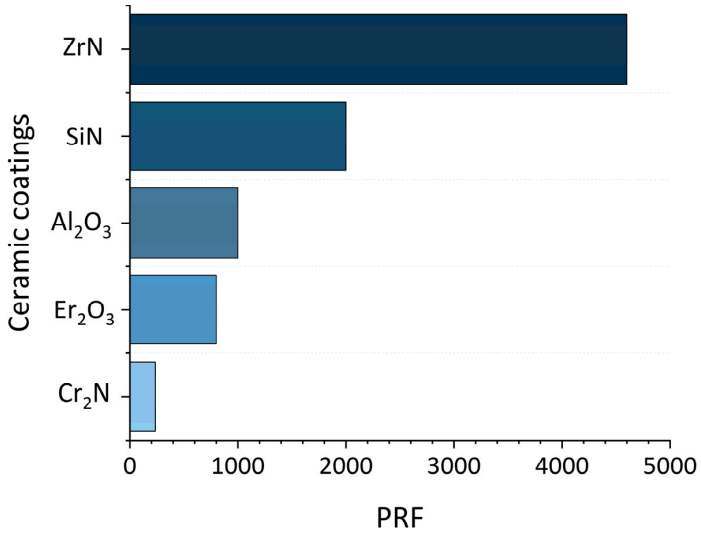

Figure 4. PRF values of ceramic coatings reported in the literature [44,59,60,62,63].

3.2. Ex Situ Surface Analytical Techniques for Evaluating HPBs' Performance

The development of suitable coatings as hydrogen permeation barriers requires controlling the microstructure of the films to optimize the properties of technological interest. The combination of in situ electrochemical tests (mentioned above) and ex situ surface analytical techniques is fundamental for understanding the performance of the HB [9]. A list of analytical techniques commonly use for evaluating HPBs' performance is reported in Table 1.

As the coating's morphology and homogeneity is of utmost importance for its effectiveness as a barrier, substrate surface preparation is essential for a good coating deposition and in order to avoid the presence of microscopic defects that are one of the main issues in gas transport [64,65].

Generally, three substrate pretreatments are performed: mechanical pretreatment (e.g., grinding, polishing), wet chemical cleaning in an ultrasonic bath, and ion etching in a vacuum chamber [64]. The main problem caused by the substrate's pretreatments is the possible formation of small pits (or cavities) in the substrate that can lead to the formation of a pinholes in the coating [66,67].

Metallographic microscopes and scanning electron microscopes (SEMs) are generally used to analyze the surface morphology of the coating, allowing the observation of cracks, pores, pinholes and other different microstructure defects, and they can give information about the grain's fine structure, allowing the determination of the particle size and the thickness of the coating [68–72]; in addition, atomic force microscopy (AFM) can be used to obtain information about the roughness of the coating, providing guidance on the development of suitable surface coating deposition methods [68–71]. Another fundamental surface analytical technique for evaluating the performance of HPBs is X-ray photoelectron spectroscopy (XPS). This technique provides information on the chemical composition and elemental distribution of the sample surface both before and after deposition of the coating, giving further insight into the quality of the deposition method [73–75].

Angle-resolved X-ray photoelectron spectroscopy (ARXPS) is a non-destructive method that can be applied for determining in-depth composition profiles of nano-sized thin films [76,77]. This method gives essential information about the mechanism of surface film formation and about the properties of the coating in terms of corrosion and wear resistance [76,77]. Scorciapino et al. [77], based on a combination of electrochemical and surface analytical studies, proposed a model for the protective properties of 20 μm Ni-P coated mild steel samples when immersed in a sulfate solution at pH 6.3. The surface of the

Ni-P coating showed a multilayer structure with different thicknesses and compositions (Figure 5a): an outermost contamination layer made of organic carbon and oxygen, a second thin layer (about 1 nm thick) made of nickel polyphosphate, a highly phosphorus-enriched interface zone of about 2 nm thick with a marked concentration gradient, and the bulk of the alloy. Figure 5b shows the reconstructed depth profile obtained by combining the maximum entropy method (MEM) with the ARXPS data of a Ni18P alloy after 1 h polarization at +0.1 V SCE in 0.1 M Na_2SO_4 [75]. The nickel–polyphosphate layer detected at the surface might act as a barrier at the surface of the alloy and hinders the dissolution of nickel ions, explaining the excellent tribological properties of Ni-P alloys and their excellent corrosion resistance.

Another interesting and increasingly used analytical technique for characterizing multilayer systems is hard X-ray photoelectron spectroscopy (HAXPES) [78,79]. A recent work [80] showed that the combination of XPS/HAXPES with Elastic Recoil Detection Analysis (ERDA) and Rutherford Backscattering Spectroscopy (RBS) allowed for studying the effect of hydrogen incorporation on alumina films (grown on silicon substrates by atomic layer deposition) and on the local chemical binding state of Al, O and H.

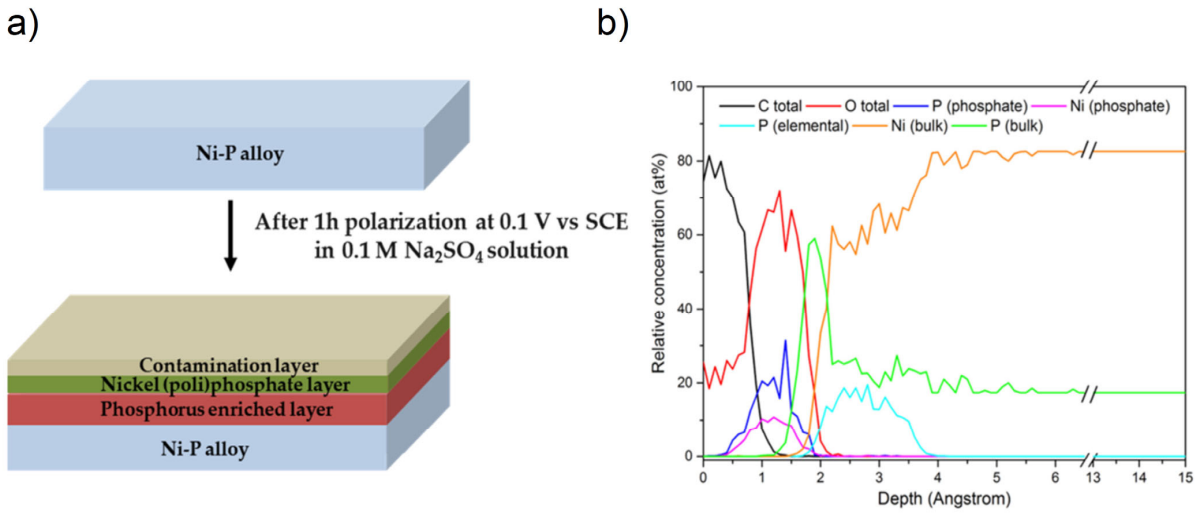

Figure 5. (**a**) Scheme of Ni-P surface layers that act as protective layers against corrosion and (**b**) MEM reconstructed depth profile of a Ni18P alloy after 1 h polarization at +0.1 V SCE in 0.1 M Na_2SO_4, adapted from [77].

Table 1. List of analytical techniques for evaluating HPBs performance.

	Technique	Information	References
In situ	Gas permeation test	Diffusion coefficient; permeability coefficient; hydrogen solubility coefficient; permeation reduction factor	[44,47–49,71]
	Devanathan–Stachurski's (D-S) cell Electrochemical test	Diffusion coefficient; trap density; subsurface concentration of hydrogen; permeation reduction factor	[50–53]
Ex situ	OM	Morphology; particle size	[64,70]
	SEM	Information about the topography, chemical composition, and film thickness (combined with EDS); 2D detailed images	[64,66–72]
	AFM	Topography; surface roughness	[64,68,71]
	XPS/ARXPS/HAXPES	Information about chemical composition, chemical state identification and film thickness; qualitative and quantitative analysis; imaging/mapping.	[65,71,73–80]
	ERDA/RBS	H-concentration in films	[80]

3.3. Production of Electroless Ni-P Coatings

To deposit a good coating, substrate pretreatment (cleaning, polishing) is important (see Section 3.2). Electroless Ni-P (ENP) plating is commonly applied as an anti-corrosion coating (e.g., for steel) [30,32], but it is currently of interest due to its low hydrogen permeability [35,81,82]. The advantage of Ni-P electroless coatings is not only the anti-corrosion properties but also the lower cost of the synthesis [30,32,35,77,81,83] compared to other coatings. The process of electrolytic nickel plating, for example, requires an external electric current, is time-consuming, and results in a less uniform coating. The great advantage of electroless coating is that it can be applied uniformly to any surface, regardless of the complexity of the surface geometry of the item to be coated, so it could also be applied to existing pipelines [28,84,85]. In addition, electroless Ni-P coating is reported to be harder and to possess higher corrosion resistance than those obtained through electrodeposition [86,87].

Various conditions are reported in the literature that are commonly adopted for electroless coatings [30,35,82,84]. In general, the main requirements for electroless Ni-P deposition are [83]:

- Source of Ni^{2+} ions: e.g., nickel sulfate or nickel chloride;
- Reducing agent: usually sodium hypo-phosphite (NaH_2PO_2);
- Complexing agents: as organic acids or their salts (acetic, malic, succinic, or citric). They prevent the formation of an excessive concentration of free metal ions, and they act as buffers and to delay the precipitation of nickel phosphite. These complexing agents exert a significant influence on the deposits' quality and porosity levels;
- Stabilizers or accelerators: they are added in small amounts (ppm) in order to raise the deposition rate. The most common stabilizers used are Pb, As, Mo, Cd ions, malic, and thioureas;
- Temperature: it influences the kinetics and speed of deposition and it must be controlled to obtain a high-quality coating. The optimum operating temperature of an acid hypophosphite plating solution ranges from 85 °C to 90 °C. High temperatures beyond 90 °C might lead to solution "plate-out" or bath decomposition [28,88];
- pH regulator: pH is an important parameter since it affects the phosphorus content: the higher the pH value, the lower the phosphorus content obtained. The common pH regulators used are sodium hydroxide and/or sulfuric acid.

The properties of the electroless Ni-P coating are mainly dependent on the content of phosphorus that controls their microstructures [89]. Based on the phosphorus content, Ni-P alloys can be divided into three groups: low (1–5 wt.%), medium (5–9 wt.%) and high (above 9 wt.%) phosphorus content [90]. The low phosphorus deposits are either crystalline or consist of a microcrystalline nickel phase [91–93]; the medium phosphorus coatings are either fully amorphous or contain mixtures of microcrystalline nickel and amorphous phases [92,94]; and at a high phosphorus concentration of about 10 wt.% (c.a. 20 at.%), the structure is X-ray amorphous [86,89–91]. The control of the plating parameters, namely the phosphorous acid concentration, temperature and time, allow for obtaining different Ni-P coatings containing various concentrations of phosphorous, and thus, different crystal structures [27,33,95–98].

3.4. Properties of Electroless Ni-P Coatings

Ni-P as protective coatings against corrosion have been studied since 1946 [99,100]. These coatings can be applied on different substrates, and they can provide excellent chemical and mechanical properties, such as adhesion, good corrosion resistance, high hardness and wear resistance [101–104].

The ISO 4527:2003 [105] lists the different requirements and test methods for analyzing specific properties of the electroless nickel–phosphorus alloy depending on the application.

In addition to the uniformity, morphology and chemical composition, other parameters such as the layer thickness, adhesion and porosity, should be evaluated for optimizing the properties of Ni-P coatings [103]. The minimum coating thickness required for corrosion resistance in service, applied on a ferrous substrate, ranges from 0.1 µm, for very mild service conditions (e.g., for thin film resistors), to 125 µm, for high severe conditions (e.g., for oil field applications) [103,105].

The upgrading of the adhesion, hardness and wear resistance of electroless Ni-P coatings can be achieved by applying a heat treatment [105]. For improving the adhesion onto steel, for example, a temperature range of 180 °C–200 °C for 2–4 h is required. In general, after the heating procedure, the hardness increases with a decrease of the phosphorus content. Heat treatment below 200 °C performed to minimize the risk of hydrogen embrittlement should not substantially increase the wear and corrosion resistance and/or the hardness of the coating. However, a temperature above 260 °C should lead to a magnetic coating.

One of the most important parameters to examine is the porosity: nickel–phosphorus coatings should be free of porosity as the corrosive processes can occur at through-thickness pores or microstructure defects [103,105]. ISO 4527:2003 [105] recommends a roughness value $R_a < 0.2$ µm to prevent corrosion. A low porosity is even more relevant when using these alloys as HPB, as the porosity affects hydrogen diffusion [106].

3.5. Nickel and Ni-P Coatings as Hydrogen Permeation Barriers

Permeability and diffusion of hydrogen through iron and iron-based alloys is high, even at room temperature, and the risk of hydrogen embrittlement is critical. Thus, the steel parts have to be protected by suitable coatings that reduce or avoid hydrogen permeation into the steel. Various hydrogen barrier coatings have been studied, including metals and alloys, oxides, ceramics, etc. [8,9,41,81]. Among these different coating materials, electrodeposited nickel and electroless nickel–phosphorus alloys are promising candidates due to their low hydrogen permeability [35,81,82,107–116].

3.5.1. Pure Nickel

Hydrogen diffusion of pure nickel was studied by Tanabe et al. [109]. Specimens of 2.1 cm diameter and thickness from 0.275 to 1.02 mm were annealed in vacuum at about 650 °C for 25 h before the tests that were performed in a temperature range from 350 to 600 °C. The diffusion coefficient of hydrogen D_{eff} was found as $7.11 \times 10^{-3} \exp(-10{,}700/RT)$ cm^2s^{-1}, and for room temperature, a value of 9.5×10^{-5} cm^2s^{-1} can be extrapolated. This value is in good agreement with results of a review of Robertson where D_{eff} is reported to be 1.33×10^{-4} cm^2s^{-1} [110].

3.5.2. Electrodeposited Nickel (ED)

Electrodeposition of nickel is performed by application of a galvanostatic current in a plating bath [86]. The effect of nickel coatings on the permeation of hydrogen through iron membranes showed a reduction of the permeation current between a factor of 10 for 3.2 µm electroless and a factor of 20 for 12.4 µm electrodeposited nickel coatings [111]. The hydrogen permeability of electrodeposited nickel on 50 µm thick AISI 1017 steel samples was studied by Paatsch [112] to correlate the coating morphology with the hydrogen diffusion coefficient. The diffusion coefficient was in the range of 5×10^{-8} to 8×10^{-8} cm^2s^{-1} for a plating current density from 0.05 to 1 mA/m^2. Kim et al. [113] studied hydrogen permeation through AISI 4340 steel covered with an electroplated nickel layer. The diffusion coefficient of the Ni layer was found in the range of $3.9 \pm 0.6 \times 10^{-9}$ cm^2s^{-1} for 5 µm to $1.4 \pm 0.4 \times 10^{-9}$ cm^2s^{-1} for a 15 µm layer (Figure 6). Results of other studies [107] are included in Table 2. The hydrogen permeation behavior of polycrystalline nickel implanted with He, Ar, Ni, Yt and Pt was also investigated [117] to elucidate the effect of surface

modification. It was found that the effective diffusion coefficient of hydrogen was lower, and the effective solubility was larger in Ni, Yt and Pt-implanted nickel with a dose of more than 1 1015 ions cm^{-2} compared to un-implanted nickel.

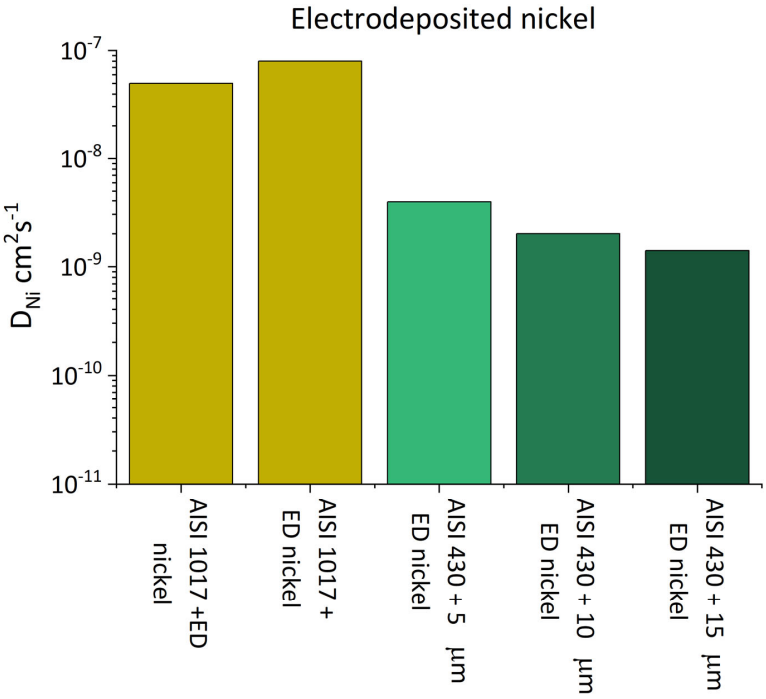

Figure 6. Diffusion coefficient values of nickel layer for electrodeposited nickel (ED) on 50 µm thick AISI 1017 steel samples reported in [111] and diffusion coefficient values of 5 µm, 10 µm and 15 µm thick electroplated nickel (ED) layers on AISI 4340 steel reported in [112].

Table 2. Effective diffusion coefficients of coated samples (D_{eff}), diffusion coefficients of the coating (D_{coat}) and subsurface concentration of hydrogen (C_0) reported in the literature for pure nickel and for electrodeposited nickel (ED) and electroless Ni-P coated steel (EN).

Material	Coating	Thickness µm	D_{eff} cm^2s^{-1}	D_{Ni} cm^2s^{-1}	C_0	Reference
Nickel	-	-	9.5×10^{-5}	-	-	[109]
	-	-	1.33×10^{-4}			[110]
AISI 1017	ED nickel	50		5.0×10^{-8}		[112]
	ED nickel	50		8.0×10^{-8}		
AISI 430	-	-	1.2×10^{-6}	-	6.9×10^{-6}	[113]
	ED nickel	5	5.0×10^{-7}	3.9×10^{-9}	4.8×10^{-6}	
	ED nickel	10	2.2×10^{-7}	2.0×10^{-9}	4.8×10^{-6}	
	ED nickel	15	8.4×10^{-8}	1.4×10^{-9}	4.8×10^{-6}	
Mild steel	-	-	1.04×10^{-6}	-		[107]
	ED nickel	8	6.78×10^{-7}	1.9×10^{-8}		
	EN nickel	6	1.38×10^{-7}	$1.2–2.4 \times 10^{-9}$		
	EN nickel	16	1.10×10^{-7}			
Ni81P19	Ribbon	38	-	3×10^{-10}		[115]
Ni81P19	Ribbon			9×10^{-11}	1823×10^{-6}	[116]
X70 steel	-	-	0.75×10^{-6}	-		[108]
	ED nickel	3.8	0.54×10^{-6}	* 4.7×10^{-9}		
	EN nickel	3.5	0.39×10^{-6}	* 2×10^{-9}		
	EN nickel	8.5	0.042×10^{-6}	* 2.7×10^{-10}		

* calculated with Equation (9).

3.5.3. Amorphous or Electroless Nickel–Phosphorus

Amorphous Ni81P19 alloys prepared by rapid quenching were tested early with respect to hydrogen permeation [115,116] and the effective hydrogen diffusion coefficient D_{eff} determined with the break-through method from the permeation curves was found to be in the order of 10^{-10} cm^2s^{-1} (Table 1) and thus very promising for a hydrogen permeation barrier. Electroless nickel–phosphorous coatings on X70 steel were studied by Samantha et al. [35,81,108] mainly for their wear resistance. A thorough characterization of the coatings was performed [81,108] and the resistance to hydrogen embrittlement of the steel/coating systems was evaluated. The effective diffusion coefficient of the steel/coating systems was calculated from the breakthrough times of the hydrogen permeation curves reported earlier [35,81]. The resulting effective diffusion coefficients D_{eff} [108] for the uncoated steel, the Ni-electroplated steel and the electroless nickel EN Ni-P coated steel are all reported in the range from 0.75 to 0.18 × 10^{-6} cm^2s^{-1} (Table 2); no attempts were made by the authors to estimate the true diffusion coefficient D_{coat} of the electroless Ni-P coating, and the values given in Table 2 for ref [108] were calculated in this work. In Figure 7, a comparison of the diffusion coefficient values of EN nickel layers (D_{Ni}) is reported.

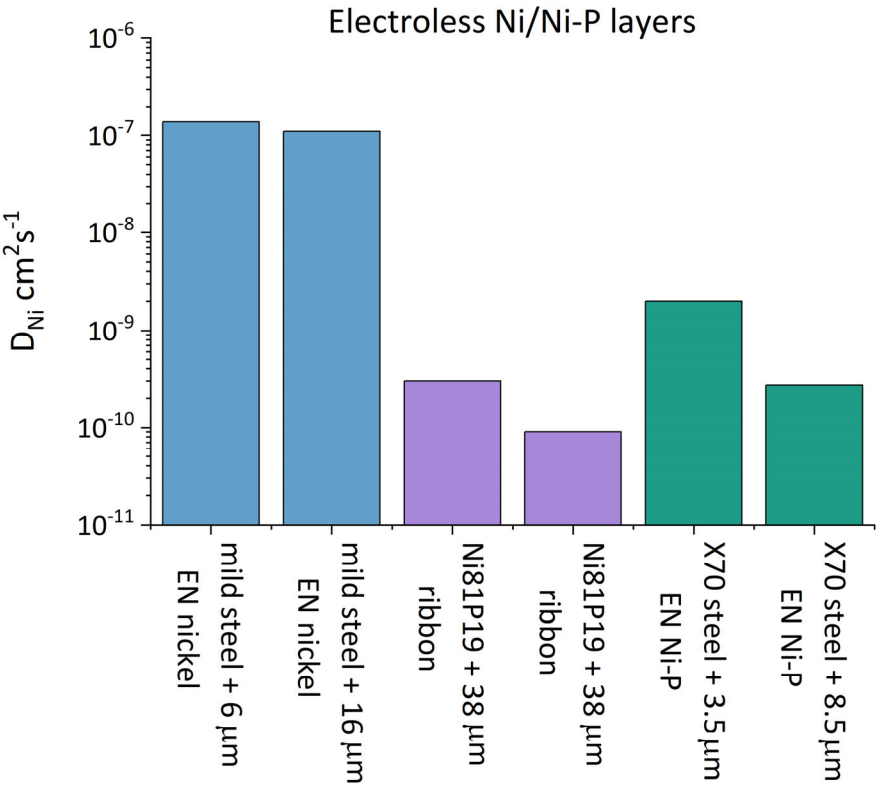

Figure 7. Comparison of the diffusion coefficient values of electroless nickel and Ni-P (EN) layers calculated starting from data reported in [107,108,115,116].

For a multilayer system, in addition to the PRF value calculated by Equation (9), considering the permeability values, the diffusion coefficient of the coating can be estimated taking into account the effective diffusion coefficients of a steel/coating system and the thickness of the substrate and the coating (Table 1), with the equation proposed in [107]:

$$\frac{L_{coat}}{D_{coat}} + \frac{L_{steel}}{D_{steel}} = \frac{L_{tot}}{D_{eff}} \quad (10)$$

where,

L_{coat}: is the thickness of the coating (μm)
L_{steel}: is the thickness of the steel substrate (μm)
L_{tot}: is the thickness of the coated sample (μm)
D_{coat}: is the diffusion coefficient of the coating (cm^2s^{-1})
D_{steel}: is the diffusion coefficient of the steel substrate (cm^2s^{-1})
D_{eff}: is the effective diffusion coefficient of the coated sample (cm^2s^{-1})

The diffusion coefficients of the electrodeposited nickel coatings vary between 4.7×10^{-9} cm^2s^{-1} for 3.8 μm and 1.4×10^{-9} cm^2s^{-1} for 15 μm coating thicknesses (Table 2). The diffusion coefficients of the electroless deposited nickel–phosphorous coatings are in the range from 2×10^{-9} to 2.7×10^{-10} cm^2s^{-1}, reaching the values of the melt spun $Ni_{81}P_{19}$ ribbons (0.9–3 $\times 10^{-10}$ cm^2s^{-1}), acting as an efficient hydrogen permeation barrier.

3.6. Application for Hydrogen Distribution Pipelines

Hydrogen pipelines have been operating worldwide for many decades with a good safety record. These pipelines are typically used for transporting hydrogen or syn gas to petrochemical plants over short distances and at low pressures [118]. However, this experience cannot be extrapolated to long distances and high pressure for the future energy demand. A large and distributed network of already existing gas pipeline infrastructure, especially in Europe [119], can serve as a possible transportation method that can be repurposed for hydrogen transportation service, whether for pure or blended gaseous hydrogen. The cost for this repurposing is estimated at 10–35% of new construction costs [120]. A summary of possible liners and coatings is presented in [118].

Among the different technological solutions, electroless nickel–phosphorus coatings are mentioned. Electroless plated nickel coating is a commercial product that results in a uniform nickel–phosphorus layer that has been successfully used as an internal coating on pipelines and fittings to improve its corrosion resistance and anti-wear properties [27]. The advantage compared to electrodeposited commercial nickel coatings is that the autocatalytic nature of the deposition does not require passing an electric current through the bath and the substrate. Electroless plating creates a uniform metal layer regardless of surface geometry. In a review it is stated [118]: "The flexibility in plating volume and thickness, ability to achieve a bright finish with minimal surface roughness, and the mature application methods make electroless plating a candidate for hydrogen pipeline coatings". It can be imagined that the process of electroless plating could be applied "in situ" in existing pipelines, using and adapting the mature technology of the "pig batch method". This is a procedure used for coating existing pipelines or for new pipelines, post-construction, that require a continuous and consistent coating [121].

4. Summary, Perspectives, and Prospects

In this review, an overview of the mechanism of hydrogen permeation, the in situ and ex situ analytical techniques, and the analytical methods that can be applied for evaluating the performance of HPBs are reported. The focus is on the properties of the electroless Ni-P coating as a HPB by reporting on the findings so far in the literature.

A literature review is provided on combining in situ and ex situ techniques to evaluate the performance of different materials such as HPB. Different methods can be used to obtain information on hydrogen permeability, solubility, and diffusion from gaseous and electrochemical permeation tests. For example, ex situ techniques can provide information on the morphology, topography, thickness, and chemical composition of the material before and after permeation tests, which helps in understanding the possible mechanisms involved in hydrogen diffusion.

Electroless Ni-P coating has been studied since 1946 as a protective coating against corrosion. It can be applied uniformly to different substrates (regardless of the geometry), and it can provide excellent chemical and mechanical properties, such as strong adhesion, good corrosion resistance, high hardness and good wear resistance. In addition, a free-pores morphology is expected for these coatings: the porosity, indeed, is an important parameter that can affect the diffusion coefficient.

Although few works have been reported in the literature regarding the use of this coating as a HPB, recent investigations suggest that they might act as an efficient hydrogen permeation barrier: the diffusion coefficient of electroless deposited nickel–phosphorous coatings is in the range from 2×10^{-9} to 2.7×10^{-10} cm^2s^{-1}, reaching the values of melt spun $Ni_{81}P_{19}$ ribbons ($0.9–3 \times 10^{-10}$ cm^2s^{-1}).

Given the excellent properties of these coatings and their ease of production, one can imagine that the electrodeposition process could be applied "in situ" in existing pipelines, using and adapting the mature technology of the "pig batch method". For these reasons, further investigations would be necessary and interesting in order to optimize the performance of electroless Ni-P coating as a hydrogen permeation barrier, with a view to future applications in hydrogen distribution lines.

Author Contributions: Conceptualization, D.B., B.E. and A.R.; investigation, D.B., B.E. and A.R.; resources, D.B., B.E. and A.R.; data curation, D.B., B.E. and A.R.; writing—original draft preparation, D.B.; writing—review and editing, B.E. and A.R.; supervision, A.R., funding acquisition, A.R. All authors have read and agreed to the published version of the manuscript.

Funding: This research was funded by the European Union NextGenerationEU under the National Recovery and Resilience Plan (NRRP) of Ministero dell'Università e della Ricerca (MUR), Project code PE0000021, Network 4 Energy Sustainable Transition, NEST.

Data Availability Statement: Not applicable.

Conflicts of Interest: The authors declare no conflicts of interest.

Abbreviations

The following abbreviations are used in this manuscript:

ARXPS	Angle-resolved X-ray photoelectron spectroscopy
AFM	Atomic force microscopy
C_0	Subsurface hydrogen concentration
CE	Counter electrode
D_{coat}	Diffusion coefficient of the coating
D_{eff}	Effective diffusion coefficient
D_{steel}	Diffusion coefficient of the steel substrate
D-S	Devanathan–Stachurski
E_D	Energy diffusion
ED	Electrodeposited
EN	Electroless
ERDA	Elastic recoil detection analysis
F	Faraday constant
HAXPES	Hard X-ray photoelectron spectroscopy
HE	Hydrogen embrittlement
HP	Hydrogen permeability
HPB	Hydrogen permeation barrier
i_{ss}	Steady-state permeation current density
J	Hydrogen diffusion flux

L_{coat}	Thickness of the coating
L_{steel}	Thickness of the steel substrate
L_{tot}	Thickness of the coated sample
MEM	Maximum entropy method
M_H	Molar mass of hydrogen
Ni-P	Nickel–phosphorous
OM	Optical microscopy
P_m	Hydrogen permeability
PRF	Permeation reduction factor
RBS	Rutherford backscattering spectroscopy
RE	Reference electrode
S	Solubility
SEM	Secondary electron microscopy
WE	Working electrode
XPS	X-ray photoelectron spectroscopy
ΔHs	Standard enthalpy of dissolution
ρ_{Fe}	Iron density

References

1. Amir, M.; Deshmukh, R.G.; Khalid, H.M.; Said, Z.; Raza, A.; Muyeen, S.M.; Nizami, A.-S.; Elavarasan, R.M.; Saidur, R.; Sopian, K. Energy Storage Technologies: An Integrated Survey of Developments, Global Economical/Environmental Effects, Optimal Scheduling Model, and Sustainable Adaption Policies. *J. Energy Storage* **2023**, *72*, 108694. [CrossRef]
2. Mazloomi, K.; Gomes, C. Hydrogen as an Energy Carrier: Prospects and Challenges. *Renew. Sustain. Energy Rev.* **2012**, *16*, 3024–3033. [CrossRef]
3. Stolten, D. *Hydrogen and Fuel Cells: Fundamentals, Technologies and Applications*; John Wiley & Sons: Weinheim, Germany, 2010; ISBN 978-3-527-32711-9.
4. Stolten, D.; Emonts, B. *Hydrogen Science and Engineering, 2 Volume Set: Materials, Processes, Systems, and Technology*; John Wiley & Sons: Weinheim, Germany, 2016; ISBN 978-3-527-33238-0.
5. Ustolin, F.; Campari, A.; Taccani, R. An Extensive Review of Liquid Hydrogen in Transportation with Focus on the Maritime Sector. *J. Mar. Sci. Eng.* **2022**, *10*, 1222. [CrossRef]
6. Meda, U.S.; Bhat, N.; Pandey, A.; Subramanya, K.N.; Lourdu Antony Raj, M.A. Challenges Associated with Hydrogen Storage Systems Due to the Hydrogen Embrittlement of High Strength Steels. *Int. J. Hydrogen Energy* **2023**, *48*, 17894–17913. [CrossRef]
7. Abohamzeh, E.; Salehi, F.; Sheikholeslami, M.; Abbassi, R.; Khan, F. Review of Hydrogen Safety during Storage, Transmission, and Applications Processes. *J. Loss Prev. Process Ind.* **2021**, *72*, 104569. [CrossRef]
8. Wetegrove, M.; Duarte, M.J.; Taube, K.; Rohloff, M.; Gopalan, H.; Scheu, C.; Dehm, G.; Kruth, A. Preventing Hydrogen Embrittlement: The Role of Barrier Coatings for the Hydrogen Economy. *Hydrogen* **2023**, *4*, 307–322. [CrossRef]
9. Li, Y.; Barzagli, F.; Liu, P.; Zhang, X.; Yang, Z.; Xiao, M.; Huang, Y.; Luo, X.; Li, C.; Luo, H.; et al. Mechanism and Evaluation of Hydrogen Permeation Barriers: A Critical Review. *Ind. Eng. Chem. Res.* **2023**, *62*, 15752–15773. [CrossRef]
10. Goyal, A.; Pouya, H.S.; Ganjian, E.; Claisse, P. A Review of Corrosion and Protection of Steel in Concrete. *Arab. J. Sci. Eng.* **2018**, *43*, 5035–5055. [CrossRef]
11. He, K.; Wang, L. A Review of Energy Use and Energy-Efficient Technologies for the Iron and Steel Industry. *Renew. Sustain. Energy Rev.* **2017**, *70*, 1022–1039. [CrossRef]
12. Mousa, E.; Wang, C.; Riesbeck, J.; Larsson, M. Biomass Applications in Iron and Steel Industry: An Overview of Challenges and Opportunities. *Renew. Sustain. Energy Rev.* **2016**, *65*, 1247–1266. [CrossRef]
13. Amezhnov, A.V.; Rodionova, I.G.; Batsalev, A.I.; D'yakonov, D.L.; Shaposhnikov, N.G.; Shatskii, T.E.; Marzoeva, M.E. Effect of Chemical Composition and Microstructure Parameters on Carbon and Low-Alloy Steel Corrosion Resistance Under Oil Industry Pipeline Operation Conditions. *Metallurgist* **2019**, *62*, 1030–1038. [CrossRef]
14. Suzuki, A.; Yukawa, H.; Murata, Y. Consistent Description of Hydrogen Permeation through Metal Membrane Based on Hydrogen Chemical Potential and Its Application to Alloy Design. *J. Mater. Res.* **2017**, *32*, 227–238. [CrossRef]
15. Nanninga, N.E.; Levy, Y.S.; Drexler, E.S.; Condon, R.T.; Stevenson, A.E.; Slifka, A.J. Comparison of Hydrogen Embrittlement in Three Pipeline Steels in High Pressure Gaseous Hydrogen Environments. *Corros. Sci.* **2012**, *59*, 1–9. [CrossRef]
16. Nanninga, N.; Slifka, A.; Levy, Y.; White, C. A Review of Fatigue Crack Growth for Pipeline Steels Exposed to Hydrogen. *J. Res. Natl. Inst. Stand. Technol.* **2010**, *115*, 437–452. [CrossRef] [PubMed]

17. Somerday, B.; Sofronis, P.; Jones, R.H. *Effects of Hydrogen on Materials: Proceedings of the 2008 International Hydrogen Conference, September 7–10, 2008, Jackson Lake Lodge, Grand Teton National Park, Wyoming, USA*; ASM International: Almere, The Netherlands, 2009; ISBN 978-1-61503-136-8.
18. Ghosh, G.; Rostron, P.; Garg, R.; Panday, A. Hydrogen Induced Cracking of Pipeline and Pressure Vessel Steels: A Review. *Eng. Fract. Mech.* **2018**, *199*, 609–618. [CrossRef]
19. Symons, D.M. A Comparison of Internal Hydrogen Embrittlement and Hydrogen Environment Embrittlement of X-750. *Eng. Fract. Mech.* **1999**, *68*, 751–771.
20. Flis, J. (Ed.) *Corrosion of Metals and Hydrogen-Related Phenomena—Selected Topics*; Materials Science Monographs; Elsevier: Amsterdam, The Netherlands, 1991; Volume 59; ISBN 978-0-444-98793-8.
21. Wach, S.; Miodownik, A.P.; Mackowiak, J. The Diffusion of Hydrogen through Pure Iron Membranes. *Corros. Sci.* **1966**, *6*, 271–285. [CrossRef]
22. Nelson, H.G. *Hydrogen Embrittlement Testing*; ASTM Special Technical Publication; American Society for Testing and Material: West Conshohocken, PA, USA, 1974; Volume 543.
23. Capelle, J.; Gilgert, J.; Dmytrakh, I.; Pluvinage, G. Sensitivity of Pipelines with Steel API X52 to Hydrogen Embrittlement. *Int. J. Hydrogen Energy* **2008**, *33*, 7630–7641. [CrossRef]
24. Hardie, D.; Charles, E.A.; Lopez, A.H. Hydrogen Embrittlement of High Strength Pipeline Steels. *Corros. Sci.* **2006**, *48*, 4378–4385. [CrossRef]
25. Zhang, L.; Imade, M.; An, B.; Wen, M.; Iijima, T.; Fukuyama, S.; Yokogawa, K. Internal Reversible Hydrogen Embrittlement of Austenitic Stainless Steels Based on Type 316 at Low Temperatures. *ISIJ Int.* **2012**, *52*, 240–246. [CrossRef]
26. Benassi, G. Critical Analysis of Hydrogen Permeation Techniques. Application to Different Steel Microstructures. Master's Thesis, Politecnico di Milano, Milano, Italy, 2013. Available online: www.politesi.polimi.it (accessed on 4 February 2025).
27. Sudagar, J.; Lian, J.; Sha, W. Electroless Nickel, Alloy, Composite and Nano Coatings—A Critical Review. *J. Alloys Compd.* **2013**, *571*, 183–204. [CrossRef]
28. Loto, C.A. Electroless Nickel Plating—A Review. *Silicon* **2016**, *8*, 177–186. [CrossRef]
29. Mindivan, F.; Mindivan, H.; Bayram, A. The Electroless Monolayer and Duplex Ni–B and Ni–P Coatings for 316L Stainless Steel in Synergistic Combination of Mechanical (Wear) and Chemical (Corrosion) Processes. *Adv. Eng. Mater.* **2023**, *25*, 2201501. [CrossRef]
30. Crobu, M.; Scorciapino, A.; Elsener, B.; Rossi, A. The Corrosion Resistance of Electroless Deposited Nano-Crystalline Ni–P Alloys. *Electrochim. Acta* **2008**, *53*, 3364–3370. [CrossRef]
31. Elsener, B.; Crobu, M.; Scorciapino, M.A.; Rossi, A. Electroless Deposited Ni–P Alloys: Corrosion Resistance Mechanism. *J. Appl. Electrochem.* **2008**, *38*, 1053–1060. [CrossRef]
32. Elsener, B.; Atzei, D.; Krolikowski, A.; Rossi, A. Effect of Phosphorus Concentration on the Electronic Structure of Nanocrystalline Electrodeposited Ni–P Alloys: An XPS and XAES Investigation. *Surf. Interface Anal.* **2008**, *40*, 919–926. [CrossRef]
33. Elsener, B.; Atzei, D.; Krolikowski, A.; Rossi Albertini, V.; Sadun, C.; Caminiti, R.; Rossi, A. From Chemical to Structural Order of Electrodeposited Ni22P Alloy: An XPS and EDXD Study. *Chem. Mater.* **2004**, *16*, 4216–4225. [CrossRef]
34. He, Y.P.; Liu, G.M.; Duan, X.H.; Wu, T.; Dong, M.; Zhu, Y.B. Effects of Nanocrystals on Hydrogen Permeation and Diffusion in Amorphous Electroless Ni-P Coatings. *Mater. Today Commun.* **2024**, *40*, 109499. [CrossRef]
35. Samanta, S.; Mondal, K.; Dutta, M.; Singh, S.B. Electroless NiP Coatings over API X70 Steel: Effect of Composition on the H-Permeation and Corrosion Resistance. *Surf. Coat. Technol.* **2021**, *409*, 126928. [CrossRef]
36. Li, X.; Ma, X.; Zhang, J.; Akiyama, E.; Wang, Y.; Song, X. Review of Hydrogen Embrittlement in Metals: Hydrogen Diffusion, Hydrogen Characterization, Hydrogen Embrittlement Mechanism and Prevention. *Acta Metall. Sin.* **2020**, *33*, 759–773. [CrossRef]
37. Tamura, M. Hydrogen Permeation Characteristics of TiN-Coated Stainless Steels. *JMSE-A* **2015**, *5*, 197–201. [CrossRef]
38. Fowler, J.D.; Chandra, D.; Elleman, T.S.; Payne, A.W.; Verghese, K. Tritium Diffusion in $A1_2O_3$ and BeO. *J. Am. Ceram. Soc.* **1977**, *60*, 155–161. [CrossRef]
39. Wipf, H. Solubility and Diffusion of Hydrogen in Pure Metals and Alloys. *Phys. Scr.* **2001**, *2001*, 43. [CrossRef]
40. Kirchheim, R. Solubility and Diffusivity of Hydrogen in Complex Materials. *Phys. Scr.* **2001**, *2001*, 58. [CrossRef]
41. Rönnebro, E.C.E.; Oelrich, R.L.; Gates, R.O. Recent Advances and Prospects in Design of Hydrogen Permeation Barrier Materials for Energy Applications—A Review. *Molecules* **2022**, *27*, 6528. [CrossRef]
42. Chen, Y.-S.; Huang, C.; Liu, P.-Y.; Yen, H.-W.; Niu, R.; Burr, P.; Moore, K.L.; Martínez-Pañeda, E.; Atrens, A.; Cairney, J.M. Hydrogen Trapping and Embrittlement in Metals—A Review. *Int. J. Hydrogen Energy* **2024**. [CrossRef]
43. Hatano, Y. Permeation and Permeation Barrier. In *Tritium: Fuel of Fusion Reactors*; Tanabe, T., Ed.; Springer: Tokyo, Japan, 2017; pp. 207–229; ISBN 978-4-431-56460-7.
44. Nemanič, V. Hydrogen Permeation Barriers: Basic Requirements, Materials Selection, Deposition Methods, and Quality Evaluation. *Nucl. Mater. Energy* **2019**, *19*, 451–457. [CrossRef]
45. Fick, A. Ueber Diffusion. *Ann. Phys.* **1855**, *170*, 59–86. [CrossRef]
46. Song, R.-H.; Pyun, S. Hydrogen Permeation Through a Bilayer of Fe/Electrodeposited Ni. *J. Electrochem. Soc.* **1990**, *137*, 1051. [CrossRef]
47. Fujiwara, H.; Ono, H.; Onoue, K.; Nishimura, S. High-Pressure Gaseous Hydrogen Permeation Test Method -Property of Polymeric Materials for High-Pressure Hydrogen Devices (1)-. *Int. J. Hydrogen Energy* **2020**, *45*, 29082–29094. [CrossRef]

48. Young, K.T.; Krentz, T.M.; d'Entremont, A.L.; Vogel, E.M.; Hitchcock, D.A. Measurement of Gas-Concentration-Driven Permeation for the Examination of Permeability, Solubility, and Diffusivity in Varying Materials. *Rev. Sci. Instrum.* **2020**, *91*, 105105. [CrossRef] [PubMed]
49. Checchetto, R.; Gratton, L.M.; Miotello, A.; Cestari, C. Hydrogen Permeation Apparatus with Thermal Desorption Spectroscopy Capabilities. *Meas. Sci. Technol.* **1995**, *6*, 1605. [CrossRef]
50. Devanathan, M.a.V.; Stachurski, Z.; Tompkins, F.C. The Adsorption and Diffusion of Electrolytic Hydrogen in Palladium. *Proc. R. Soc. Lond. Ser. A Math. Phys. Sci.* **1997**, *270*, 90–102. [CrossRef]
51. Devanathan, M.a.V.; Stachurski, Z. The Mechanism of Hydrogen Evolution on Iron in Acid Solutions by Determination of Permeation Rates. *J. Electrochem. Soc.* **1964**, *111*, 619. [CrossRef]
52. Standard Practice for Evaluation of Hydrogen Uptake, Permeation, and Transport in Metals by an Electrochemical Technique. Available online: https://www.astm.org/g0148-97r18.html (accessed on 2 November 2023).
53. *ISO 17081:2004(En)*; Method of Measurement of Hydrogen Permeation and Determination of Hydrogen Uptake and Transport in Metals by an Electrochemical Technique. International Organization for Standardization: Genève, Switzerland, 2004. Available online: https://www.iso.org/obp/ui#iso:std:iso:17081:ed-1:v1:en (accessed on 8 March 2024).
54. Turnbull, A.; Carroll, M.W.; Ferriss, D.H. Analysis of Hydrogen Diffusion and Trapping in a 13% Chromium Martensitic Stainless Steel. *Acta Metall.* **1989**, *37*, 2039–2046. [CrossRef]
55. Turnbull, A.; Saenz de Santa Maria, M.; Thomas, N.D. The Effect of H_2S Concentration and pH on Hydrogen Permeation in AISI 410 Stainless Steel in 5% NaCl. *Corros. Sci.* **1989**, *29*, 89–104. [CrossRef]
56. Frappart, S.; Feaugas, X.; Creus, J.; Thebault, F.; Delattre, L.; Marchebois, H. Study of the Hydrogen Diffusion and Segregation into Fe–C–Mo Martensitic HSLA Steel Using Electrochemical Permeation Test. *J. Phys. Chem. Solids* **2010**, *71*, 1467–1479. [CrossRef]
57. Crank, J. *The Mathematics of Diffusion*; Clarendon Press: Oxford, UK, 1979; ISBN 978-0-19-853411-2.
58. Laadel, N.-E.; El Mansori, M.; Kang, N.; Marlin, S.; Boussant-Roux, Y. Permeation Barriers for Hydrogen Embrittlement Prevention in Metals—A Review on Mechanisms, Materials Suitability and Efficiency. *Int. J. Hydrogen Energy* **2022**, *47*, 32707–32731. [CrossRef]
59. Levchuk, D.; Koch, F.; Maier, H.; Bolt, H. Deuterium Permeation through Eurofer and α-Alumina Coated Eurofer. *J. Nucl. Mater.* **2004**, *328*, 103–106. [CrossRef]
60. Matějíček, J.; Veverka, J.; Nemanič, V.; Cvrček, L.; Lukáč, F.; Havránek, V.; Illková, K. Characterization of Less Common Nitrides as Potential Permeation Barriers. *Fusion Eng. Des.* **2019**, *139*, 74–80. [CrossRef]
61. Chikada, T.; Suzuki, A.; Koch, F.; Maier, H.; Terai, T.; Muroga, T. Fabrication and Deuterium Permeation Properties of Erbia-Metal Multilayer Coatings. *J. Nucl. Mater.* **2013**, *442*, S592–S596. [CrossRef]
62. Levchuk, D.; Levchuk, S.; Maier, H.; Bolt, H.; Suzuki, A. Erbium Oxide as a New Promising Tritium Permeation Barrier. *J. Nucl. Mater.* **2007**, *367–370*, 1033–1037. [CrossRef]
63. Nemanič, V.; McGuiness, P.J.; Daneu, N.; Zajec, B.; Siketić, Z.; Waldhauser, W. Hydrogen Permeation through Silicon Nitride Films. *J. Alloys Compd.* **2012**, *539*, 184–189. [CrossRef]
64. Panjan, P.; Drnovšek, A.; Gselman, P.; Čekada, M.; Panjan, M. Review of Growth Defects in Thin Films Prepared by PVD Techniques. *Coatings* **2020**, *10*, 447. [CrossRef]
65. Hannachi, R.; Biggio, D.; Elsener, B.; Fantauzzi, M.; Rossi, A. X-Ray Photoelectron Spectroscopy Investigation of X60 Steel. *Surf. Sci. Spectra* **2024**, *31*, 024014. [CrossRef]
66. Harlin, P.; Bexell, U.; Olsson, M. Influence of Surface Topography of Arc-Deposited TiN and Sputter-Deposited WC/C Coatings on the Initial Material Transfer Tendency and Friction Characteristics under Dry Sliding Contact Conditions. *Surf. Coat. Technol.* **2009**, *203*, 1748–1755. [CrossRef]
67. Panjan, P.; Drnovšek, A.; Gselman, P.; Čekada, M.; Panjan, M.; Bončina, T.; Kek Merl, D. Influence of Growth Defects on the Corrosion Resistance of Sputter-Deposited TiAlN Hard Coatings. *Coatings* **2019**, *9*, 511. [CrossRef]
68. Tench, R.J.; Chow, R.; Kozlowski, M.R. Characterization of Defect Geometries in Multilayer Optical Coatings. *J. Vac. Sci. Technol. A* **1994**, *12*, 2808–2813. [CrossRef]
69. Spalvins, T. Characterization of Defect Growth Structrures in Ion-Plated Films by Scanning Electron Microscopy. *Thin Solid Film.* **1979**, *64*, 143–148. [CrossRef]
70. Podgornik, B.; Hogmark, S.; Sandberg, O. Influence of Surface Roughness and Coating Type on the Galling Properties of Coated Forming Tool Steel. *Surf. Coat. Technol.* **2004**, *184*, 338–348. [CrossRef]
71. Shen, X.; Xu, Y.-P.; Li, H.-Z.; Yi, J.; Lyu, Y.-M.; Zhou, H.-S.; Luo, G.-N. Optimization of Alumina Tritium Permeation Barrier with Consideration of the Thickness and the Surface Coverage. *Nucl. Mater. Energy* **2024**, *38*, 101574. [CrossRef]
72. Ortiz, N.; González-Parra, J.R.; Olaya, J.; Agredo, D.; Valdez, R.; Waage, H.; Bolarín, A.M.; Sánchez, F.; Barba-Pingarrón, A. Morphological and Corrosion Characterization of Electroless Ni-P Coatings Deposited on Ductile Iron. *Coatings* **2024**, *14*, 1317. [CrossRef]
73. Krishna, D.N.G.; Philip, J. Review on Surface-Characterization Applications of X-Ray Photoelectron Spectroscopy (XPS): Recent Developments and Challenges. *Appl. Surf. Sci. Adv.* **2022**, *12*, 100332. [CrossRef]
74. Huang, N.K.; Wang, D.Z.; Xiong, Q.; Yang, B. XPS Study of Hydrogen Permeation Effect on SiC–C Films. *Nucl. Instrum. Methods Phys. Res. Sect. B Beam Interact. Mater. At.* **2003**, *207*, 395–401. [CrossRef]

75. Wang, W.; Yan, G.; Zhang, J.; Ma, Z.; Wang, L.; Guo, Z.; Zhang, S.; Wu, Y. Hydrogen Permeation Behavior of Zirconium Nitride Film on Zirconium Hydride. *Materials* **2022**, *15*, 550. [CrossRef]
76. Cumpson, P.J. Angle-Resolved XPS and AES: Depth-Resolution Limits and a General Comparison of Properties of Depth-Profile Reconstruction Methods. *J. Electron. Spectrosc. Relat. Phenom.* **1995**, *73*, 25–52. [CrossRef]
77. Scorciapino, M.A.; Fantauzzi, M.; Crobu, M.; Navarra, G.; Elsener, B.; Rossi, A. Nanostructure of Surface Films on Ni18P Alloy in Sulfate Solutions by the Maximum Entropy Method. *ACS Omega* **2017**, *2*, 7790–7802. [CrossRef] [PubMed]
78. Artyushkova, K.; Leadley, S.R.; Shard, A.G. Introduction to Reproducible Laboratory Hard X-Ray Photoelectron Spectroscopy. *J. Vac. Sci. Technol. A* **2024**, *42*, 052801. [CrossRef]
79. Cancellieri, C.; Lorenzin, G.; Lyanage, M.; Turlo, V.; Watts, J.F.; Jeurgens, L.P.H. Chemical and Electronic Structure of Buried W/Cu, W/Cr, and W/Mo Interfaces by In Situ XPS/HAXPES Auger Parameter Analysis. *Surf. Interface Anal.* **2025**, 1–11. [CrossRef]
80. Cancellieri, C.; Gramatte, S.; Politano, O.; Lapeyre, L.; Klimashin, F.F.; Mackosz, K.; Utke, I.; Novotny, Z.; Müller, A.M.; Vockenhuber, C.; et al. Effect of Hydrogen on the Chemical State, Stoichiometry and Density of Amorphous Al2O3 Films Grown by Thermal Atomic Layer Deposition. *Surf. Interface Anal.* **2024**, *56*, 293–304. [CrossRef]
81. Samanta, S.; Singh, C.; Banerjee, A.; Mondal, K.; Dutta, M.; Singh, S.B. Development of Amorphous Ni-P Coating over API X70 Steel for Hydrogen Barrier Application. *Surf. Coat. Technol.* **2020**, *403*, 126356. [CrossRef]
82. Hino, M.; Doi, Y.; Kuwano, R.; Oda, Y.; Horikawa, K. Effect of Phosphorus Content on Hydrogen Embrittlement for High Strength Steel Treated with Electroless Ni–P Plating. *Mater. Trans.* **2021**, *62*, 75–81. [CrossRef]
83. Fayyad, E.M.; Abdullah, A.M.; Hassan, M.K.; Mohamed, A.M.; Jarjoura, G.; Farhat, Z. Recent Advances in Electroless-Plated Ni-P and Its Composites for Erosion and Corrosion Applications: A Review. *Emergent Mater.* **2018**, *1*, 3–24. [CrossRef]
84. Osifuye, C.O.; Popoola, A.P.I.; Loto, C.A.; Oloruntoba, D.T. Effect of Bath Parameters on Electroless Ni-P and Zn-P Deposition on 1045 Steel Substrate. *Int. J. Electrochem. Sci.* **2014**, *9*, 6074–6087. [CrossRef]
85. Electro-Coating Electroless Nickel Plating Services | Electro-Coating. Available online: https://www.electro-coatings.com/electroless-nickel-plating.php (accessed on 4 February 2025).
86. Lelevic, A.; Walsh, F.C. Electrodeposition of NiP Alloy Coatings: A Review. *Surf. Coat. Technol.* **2019**, *369*, 198–220. [CrossRef]
87. Daly, B.P.; Barry, F.J. Electrochemical Nickel–Phosphorus Alloy Formation. *Int. Mater. Rev.* **2003**, *48*, 326–338. [CrossRef]
88. Guo, R.H.; Jiang, S.X.; Yuen, C.W.M.; Ng, M.C.F.; Lan, J.W.; Zheng, G.H. Influence of Deposition Parameters and Kinetics of Electroless Ni-P Plating on Polyester Fiber. *Fibers Polym.* **2012**, *13*, 1037–1043. [CrossRef]
89. Mousavi, M.; Rahimi, E.; Mol, J.M.C.; Gonzalez-Garcia, Y. The Effect of Phosphorous Content on the Microstructure and Localised Corrosion of Electroless Nickel-Coated Copper. *Surf. Coat. Technol.* **2024**, *492*, 131174. [CrossRef]
90. Standard Specification for Autocatalytic (Electroless) Nickel-Phosphorus Coatings on Metal. Available online: https://www.astm.org/b0733-22.html (accessed on 6 February 2025).
91. Mai, Q.X.; Daniels, R.D.; Harpalani, H.B. Structural Changes Induced by Heating in Electroless Nickel-Phosphorus Alloys. *Thin Solid Film.* **1988**, *166*, 235–247. [CrossRef]
92. Martyak, N.M. Characterization of Thin Electroless Nickel Coatings. *Chem. Mater.* **1994**, *6*, 1667–1674. [CrossRef]
93. Lambert, M.R.; Duquette, D.J. A Study of Electroless Nickel Coatings Containing Low Phosphorus. *Thin Solid Film.* **1989**, *177*, 207–223. [CrossRef]
94. Martyak, N.M.; Drake, K. Peak-Profile Analysis of Electroless Nickel Coatings. *J. Alloys Compd.* **2000**, *312*, 30–40. [CrossRef]
95. Pillai, A.M.; Rajendra, A.; Sharma, A.K. Electrodeposited Nickel–Phosphorous (Ni–P) Alloy Coating: An in-Depth Study of Its Preparation, Properties, and Structural Transitions. *J. Coat. Technol. Res.* **2012**, *9*, 785–797. [CrossRef]
96. Bredael, E.; Blanpain, B.; Celis, J.P.; Roos, J.R. On the Amorphous and Crystalline State of Electrodeposited Nickel-Phosphorus Coatings. *J. Electrochem. Soc.* **1994**, *141*, 294. [CrossRef]
97. Keong, K.G.; Sha, W. Crystallisation and Phase Transformation Behaviour of Electroless Nickel-Phosphorus Deposits and Their Engineering Properties. *Surf. Eng.* **2002**, *18*, 329–343. [CrossRef]
98. Hu, C.-C.; Bai, A. Influences of the Phosphorus Content on Physicochemical Properties of Nickel–Phosphorus Deposits. *Mater. Chem. Phys.* **2003**, *77*, 215–225. [CrossRef]
99. Brenner, A.; Riddell, G.E. Nickel Plating on Steel by Chemical Reduction. *J. Res. Natl. Bur. Stand.* **1946**, *37*, 31–34. [CrossRef]
100. Hari Krishnan, K.; John, S.; Srinivan, K.N.; Praveen, J.; Ganesan, M.; Kavimani, P.M. An Overall Aspect of Electroless Ni-P Depositions—A Review Article. *Metall. Mater. Trans. A* **2006**, *37*, 1917–1926.
101. Manna, M.; Bandyopadhyay, N.; Bhattacharjee, D. Effect of Plating Time for Electroless Nickel Coating on Rebar Surface: An Option for Application in Concrete Structure. *Surf. Coat. Technol.* **2008**, *202*, 3227–3232. [CrossRef]
102. Vitry, V.; Francq, E.; Bonin, L. Mechanical Properties of Heat-Treated Duplex Electroless Nickel Coatings. *Surf. Eng.* **2019**, *35*, 158–166. [CrossRef]
103. Mainier, F.B.; Fonseca, M.P.C.; Tavares, S.S.M.; Pardal, J.M. Quality of Electroless Ni-P (Nickel-Phosphorus) Coatings Applied in Oil Production Equipment with Salinity. *J. Mater. Sci. Chem. Eng.* **2013**, *1*, 1–8. [CrossRef]
104. Sahoo, P.; Das, S.K. Tribology of Electroless Nickel Coatings—A Review. *Mater. Des.* **2011**, *32*, 1760–1775. [CrossRef]

105. *ISO 4527:2003*; Metallic Coatings—Autocatalytic (Electroless) Nickel-Phosphorus Alloy Coatings—Specification and Test Methods. International Organization for Standardization: Genève, Switzerland, 2003. Available online: https://www.iso.org/standard/36258.html (accessed on 6 February 2025).
106. Yaktiti, A.; Dreano, A.; Carton, J.F.; Christien, F. Hydrogen Diffusion and Trapping in a Steel Containing Porosities. *Corros. Sci.* **2022**, *199*, 110208. [CrossRef]
107. Luu, W.C.; Kuo, H.S.; Wu, J.K. Hydrogen Permeation through Nickel-Plated Steels. *Corros. Sci.* **1997**, *39*, 1051–1059. [CrossRef]
108. Samanta, S.; Vishwanath, K.; Mondal, K.; Dutta, M.; Singh, S.B. Electroless Amorphous NiP Coatings Over API X70 Steel: Resistance to Wear and Hydrogen Embrittlement. *Met. Mater. Int.* **2022**, *28*, 397–411. [CrossRef]
109. Tanabe, T.; Miyata, Y.; Imoko, S. Hydrogen Permeation Through Nickel. *Technol. Rep. Osaka Univ.* **1977**, *27*, 389–396.
110. Robertson, W.M. Hydrogen Permeation, Diffusion and Solution in Nickel. *Int. J. Mater. Res.* **1973**, *64*, 436–443. [CrossRef]
111. Chatterjee, S.S.; Ateya, B.G.; Pickering, H.W. Effect of Electrodeposited Metals on the Permeation of Hydrogen through Iron Membranes. *Met. Trans. A* **1978**, *9*, 389–395. [CrossRef]
112. Paatsch, W. Morphology and Permeability of Nickel Electro-Deposits. *Plat. Surf. Finish.* **1988**, *75*, 52–55.
113. Kim, K.B.; Park, K.; Lee, J.S. Hydrogen Permeation Behavior of Nickel Electroplated AISI 4340 Steel. *Met. Mater.* **1998**, *4*, 1013–1016. [CrossRef]
114. Nishimura, R.; Okitsu, K.; Inoue, H.; Latanision, R.; Hubler, G. *Hydrogen Permeation Behavior in Polycrystalline Nickel Implanted with Various Elements*; Wit Press Limited: Cambridge, MA, USA, 2007; Volume 55, p. 51; ISBN 978-1-84564-073-6.
115. Sakamoto, Y.; Takao, K.; Baba, K. Diffusivity of Hydrogen in Amorphous Ni81P19 and Ni70Cr6.7Fe2.5Si8.0B12.8 Alloys. *Mater. Sci. Eng.* **1988**, *97*, 437–440. [CrossRef]
116. Santos, D.S.D.; Miranda, P.E.V.D. Hydrogen Solubility in Amorphous and Crystalline Materials. *Int. J. Hydrogen Energy* **1998**, *23*, 1011–1017. [CrossRef]
117. Nishimura, R.; Latanision, R.M.; Hubler, G.K. Hydrogen Permeation Behavior in Polycrystalline Nickel Implanted with Helium, Argon, Nickel, Yttrium and Platinum. *Mater. Sci. Eng.* **1987**, *90*, 243–251. [CrossRef]
118. Li, Y.; Huard, M.; Wong, K.; Wang, X.; Adane, K.F. *Coatings and Liners for Hydrogen Service Pipelines*; Canadian Standards Association: Toronto, ON, Canada, 2024. Available online: https://www.csagroup.org/article/research/coatings-and-liners-for-hydrogen-service-pipelines/?srsltid=AfmBOopIuX2eH5ywjflCYZGOvd7Dfce4HVyVg-4OFkTPjd_zYekX--Ey (accessed on 4 February 2025).
119. Lipiäinen, S.; Lipiäinen, K.; Ahola, A.; Vakkilainen, E. Use of Existing Gas Infrastructure in European Hydrogen Economy. *Int. J. Hydrogen Energy* **2023**, *48*, 31317–31329. [CrossRef]
120. Adam, P.; von dem Bussche, C.; Engelshove, S.; Thiemann, T. Hydrogen Infrastructure—The Pillar of Energy Transition. In *the Practical Conversion of Long-Distance Gas Networks to Hydrogen Operation*; Siemens Energy, Gascade Gastransport GmbH, Nowega GmbH: Munich, Germany, 2020.
121. *AMPP TR21473-2024*; In-Situ Coating of Steel Pipelines via Pigging. Association for Materials Protection and Performance: Houston, TX, USA, 2024. Available online: https://store.ampp.org/ampp-tr21473-2024-in-situ-coating-of-steel-pipelines-via-pigging (accessed on 4 February 2025).